AIP Applied Physics Letters

Thermal treatment-induced ductile-to-brittle transition of submicron-sized Si pillars fabricated by focused ion beam

Yue-cun Wang, De-gang Xie, Xiao-hui Ning, and Zhi-wei Shan

Citation: Applied Physics Letters **106**, 081905 (2015); doi: 10.1063/1.4913241
View online: http://dx.doi.org/10.1063/1.4913241
View Table of Contents: http://scitation.aip.org/content/aip/journal/apl/106/8?ver=pdfcov
Published by the AIP Publishing

Articles you may be interested in
Ductile-to-brittle transition in spallation of metallic glasses
J. Appl. Phys. **116**, 143503 (2014); 10.1063/1.4897552

Understanding the amorphous-to-microcrystalline silicon transition in SiF4/H2/Ar gas mixtures
J. Chem. Phys. **140**, 234706 (2014); 10.1063/1.4883503

Temperature-induced ductile-to-brittle transition of bulk metallic glasses
Appl. Phys. Lett. **102**, 171901 (2013); 10.1063/1.4803170

Ellipsometry investigation of the amorphous-to-microcrystalline transition in a-Si:H under hydrogen-plasma treatment
J. Appl. Phys. **107**, 083509 (2010); 10.1063/1.3393273

Electromigration induced ductile-to-brittle transition in lead-free solder joints
Appl. Phys. Lett. **89**, 141914 (2006); 10.1063/1.2358113

This article is copyrighted as indicated in the article. Reuse of AIP content is subject to the terms at: http://scitation.aip.org/termsconditions. Downloaded to IP: 117.32.153.170 On: Wed, 04 Mar 2015 00:28:44

APPLIED PHYSICS LETTERS **106**, 081905 (2015)

Thermal treatment-induced ductile-to-brittle transition of submicron-sized Si pillars fabricated by focused ion beam

Yue-cun Wang, De-gang Xie, Xiao-hui Ning, and Zhi-wei Shan[a)]
Center for Advancing Materials Performance from the Nanoscale (CAMP-Nano) and Hysitron Applied Research Center in China (HARCC), State Key Laboratory for Mechanical Behavior of Materials, Xi'an Jiaotong University, Xi'an 710049, China

(Received 26 January 2015; accepted 7 February 2015; published online 25 February 2015; corrected 3 March 2015)

Si pillars fabricated by focused ion beam (FIB) had been reported to have a critical size of 310–400 nm, below which their deformation behavior would experience a brittle-to-ductile transition at room temperature. Here, we demonstrated that the size-dependent transition was actually stemmed from the amorphous Si (a-Si) shell introduced during the FIB fabrication process. Once the a-Si shell was crystallized, Si pillars would behave brittle again with their modulus comparable to their bulk counterpart. The analytical model we developed has been proved to be valid in deriving the moduli of crystalline Si core and a-Si shell. © *2015 AIP Publishing LLC*.
[http://dx.doi.org/10.1063/1.4913241]

With the development of micro/nano-electromechanical systems (MEMS/NEMS), the deformation and fracture behaviors of micro/nanoscale Si have been the high interest of many communities because they are the basis for understanding the failure mechanism in these devices.[1–3] Bulk Si is known to be quite brittle at room temperature (RT), and the brittle-to-ductile transition (BDT) temperature of bulk Si is as high as ~600 °C.[4] In sharp contrast to their bulk counterpart, recently, Östlund *et al.*[5] reported that when the diameter of Si pillars was reduced below a critical value of 310–400 nm by focused ion beam (FIB), they would become ductile at RT. However, this size-dependent BDT is at odds with the results measured from FIB free Si samples.[6–10] For example, Deneen *et al.*[10] found that the Si nanospheres with their diameters ranging from 100–200 nm still fractured in a brittle manner in response to the compression stress at RT; Zhu *et al.*[6] and Gorden *et al.*[9] found that as-grown Si nanowires with diameters as small as 15 nm also fractured in a brittle manner when they were subjected to uniaxial tensile test and bending tests, respectively. In addition, molecular dynamics (MD) simulations suggested that the critical size for pure single crystalline Si to experience BDT at RT should be less than 4 nm.[11] These findings prompt us to surmise that the reported size-dependent BDT may not be the intrinsic property of pure single crystal Si but an outcome resulted from the imperfect sample fabrication process.

Actually, it has been well established that a FIB-affected surface layer will be created for samples prepared through FIB machining. For given materials, the thickness of this surface layer depends on the fabrication parameters, such as voltage, beam current, and incident angle. For metal based materials, it has been found that ion beam can dramatically alter the yield stress of FIB fabricated submicron-sized samples.[12,13] However, for semiconductor materials, the effect of ion beam on the mechanical behavior of FIBed samples has been largely overlooked.[5,14] One possible reason is that the majority of the reported mechanical tests on FIB-milled semiconductor pillars were carried out in scanning electron microscope (SEM) and the ion beam irradiation-affected layer cannot be recognized from the SEM image. In contrast, transmission electron microscope (TEM) is a very effective tool to identify the FIB-affected layer. Therefore, *in situ* TEM mechanical tests should be able to clarify whether the size-dependent BDT is the intrinsic property of Si or simply an outcome resulted from the imperfect sample preparation method.

For simplicity of sample preparation, we choose to use boron doped ⟨100⟩-oriented single crystal Si wedge as the starting material. This Si wedge was initially designed to facilitate the compression tests on particles inside TEM and more details about the geometry of the Si wedge can be found in references.[15,16] Submicron-sized Si pillars with their nominal diameters D (at half height) ranging from 85 nm to 650 nm and aspect ratio (height to diameter) 3–4 were fabricated directly from the wedge using a Helios NanoLab 600i dual-beam FIB system. All Si pillars reported in this work were micromachined under 30 keV with the beam current of Ga ions sequentially decreasing from 440 pA (coarse cutting) to 1.5 pA (fine polishing). The maximum current used in our work is much milder than those reported in literatures.[14,17] Both the thermal treatments and the mechanical tests were conducted with an *in situ* thermomechanical testing system manufactured by Hysitron Inc (Hysitron PI95 H1H) inside a Hitachi H9500 TEM operated at 300 kV at RT. All the mechanical tests reported in this work were run under displacement-controlled mode with the displacement rate of 5 nm/s. The loading direction was along [001], and the diameter of the flat diamond punch was ~2 μm. The engineering stress was defined as the ratio of the measured load to the nominal cross-sectional area of the pillar, and the engineering strain was defined to be the ratio of the deformation displacement of the pillar (i.e., the reading displacement subtracted the contribution from substrate) to its initial height (the distance between the top end and the substrate).

[a)]Author to whom correspondence should be addressed. Electronic mail: zwshan@mail.xjtu.edu.cn

This article is copyrighted as indicated in the article. Reuse of AIP content is subject to the terms at: http://scitation.aip.org/termsconditions. Downloaded to IP: 117.32.153.170 On: Wed, 04 Mar 2015 00:28:44

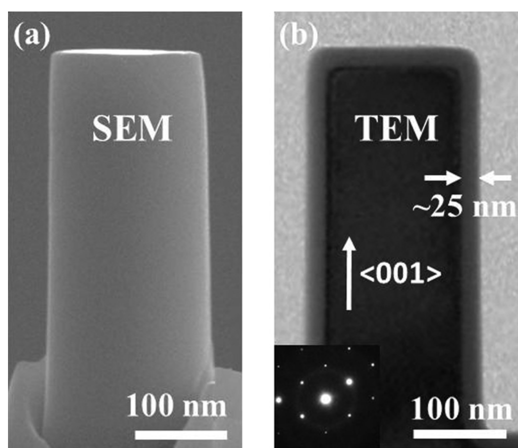

FIG. 1. Images of as-FIBed Si pillars taken with SEM (a) and TEM (b), respectively. The crystalline core and its FIB-affected amorphous shell can be seen clearly under TEM imaging condition but become invisible under SEM observation condition. The inset selected area diffraction pattern ($[0\bar{1}1]$ zone axis) in (b) is taken from the upper part of the pillar.

TEM observation found that the as-FIBed Si pillars are indeed a composite material with core-shell structure instead of being an expected single crystal sample with neglectable FIB-affected amorphous layer. One typical example is shown in Fig. 1. An as-fabricated pillar sample with its normal diameter of $D = 204$ nm exhibited uniform contrast under SEM observation (Fig. 1(a)). However, TEM observation of a sample with similar diameter (Fig. 1(b)) clearly revealed that this pillar had a shell with its thickness as high as $\sim$25 nm. Selected area diffraction pattern (inset in Fig. 1(b)) demonstrated that the shell was amorphous silicon (a-Si) and the core part was crystalline Si (c-Si). Statistic measurements found that the thickness of the a-Si shell was always about 25–30 nm, regardless of the diameter of the pillars. This value also agrees well with those reported in literatures, i.e., $\sim$28 nm for Si and $\sim$25 nm for GaAs when 30 keV Ga ions are used.[14,19–21] Calculation demonstrated that for the sample shown in Fig. 1, the a-Si occupied as high as $\sim$45% of the total volume. Similar to those reported by Östlund *et al.*,[5] uniaxial compression tests found that the pillars shown in Fig. 1 were indeed quite ductile. Then the following questions arise naturally: I. If we can crystallize the a-Si, will the pillars behave brittle again? II. Given the volume ratio of the a-Si and c-Si, can we predict the modulus of the core-shell structured pillars?

Let us first address question I. In order to crystalize the a-Si shell (Fig. 2(a)), we adopted Hysitron PI95 H1H, the first TEM compatible system to enable quantitative mechanical and thermal tests simultaneously, to treat as-fabricated Si samples. This approach was actually inspired by previous studies[18–20] which showed that the a-Si introduced by ion bombardment could be crystallized through thermal annealing. The core of the heating function of Hysitron PI95 H1H is the single crystal silica based heater (Fig. 2(b)). The highest allowed temperature for this system is about 450 °C, and the feedback control enables users to measure and control the temperature accurately. The Si wedge with FIBed Si pillars was glued on the top end of the heater (see Fig. 2(b)). When in use, the detachable heater along with the sample will be fixed to the PI95 H1H TEM holder by four copper screws which also serve as conductive connectors. The programed thermal treatment procedure reported in this work is first to heat the sample to the peak temperature of 360 °C with the heating rate of $\sim$100 °C/s, and then keep temperature at 360 °C for 10 min before cooling down to ambient temperature at the cooling rate of $\sim$10 °C/s. The current density of the electron beam used to monitor the sample evolution was about 4×10^{-2} A/cm^2. After the thermal treatment, the sample geometry kept almost unchanged. However, bright field TEM observation found that the contrast of the thermal-treated sample (Fig. 2(c)) was very different from that of the as-FIBed sample (e.g., Fig. 1(b)). Both dark field TEM image (Fig. 2(d)) and selected area diffraction pattern (Fig. 2(e), taken from the area framed by the dashed box in Fig. 2(c)) confirmed that the a-Si shell had crystallized into polycrystalline Si which has the same diamond structure as the c-Si core. It is worth noting that conventional solid-phase crystallization of a-Si films usually needs to keep the sample at $\sim$600 °C in furnace for tens of hours.[21,22] Apparently, the thermal treatment procedure used in our work is more

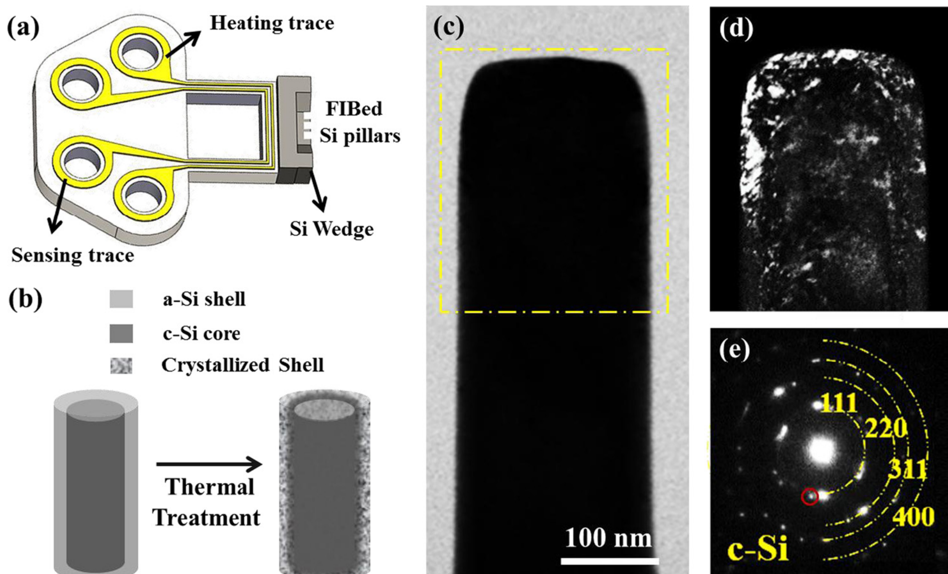

FIG. 2. Crystallization of the as-FIBed Si pillar through thermal treatment. (a) Schematic design of FIBed Si pillar before (left) and after (right) thermal treatment. (b) Schematic illustration of the Si wedge with FIBed Si pillars glued on a silica glass heating stage under feedback control. (c) Bright-field TEM image of the FIBed Si pillar after thermal treatment. (d) Dark-field TEM image of the framed zone in (c) and the corresponding selected area diffraction pattern (e). The red circled {111} diffraction spot was used to take the dark-field image in (d).

This article is copyrighted as indicated in the article. Reuse of AIP content is subject to the terms at: http://scitation.aip.org/termsconditions. Downloaded to IP: 117.32.153.170 On: Wed, 04 Mar 2015 00:28:44

efficient. One possible reason is that the c-Si core has decreased the crystallization temperature essentially by serving as the nucleation sites.

After the crystallization of the a-Si shell, the Si pillars did behave brittle again, even though their sizes are much smaller than the critical size of reported BDT.[5] One typical example is shown in Fig. 3. The diameter of this thermal-treated Si pillar is about 206 nm. During the compression test, the stress increased almost linearly with the increasing strain at the beginning (red color curve). However, a strain burst set in after the stress reached its peak value. At the same time, a vertical crack was observed to nucleate in the central of the thermal-treated pillar and then propagated downward (see Movie S1[30]). The inset framed by the red solid box is the bright filed TEM image of the thermal-treated Si pillar taken after the test. Analysis suggested that the splitting crack nucleated at the intersection of two {111} slipping planes and propagates along the ⟨100⟩ direction (axial direction of the pillar) on the {110} plane, which is the typical fracture characteristic of bulk single crystal Si. In addition, both the apparent modulus (∼125 GPa) and the fracture strength (∼7.6 GPa) of the thermal-treated Si pillar are at the same level of those of their bulk counterpart (∼130 GPa (Ref. 23) and ∼7.0 GPa (Ref. 1)). In contrast, the as-FIBed Si pillar with similar diameter (212 nm) deformed in a quite ductile manner, as evidenced by Movie S2 (Ref. 30) and the image taken after the test (inset framed by the black solid box in Fig. 3). The "softening" observed at the very beginning of the stress-strain curve of this as-FIBed Si (black curve in Fig. 3) is due to the plastic deformation of the a-Si cap (see Movie S2). The superb compression deformation ability of FIB-introduced a-Si is quite counter-intuitive because amorphous materials are usually known to be brittle at RT. Eventhough the underlying physical mechanism remains elusive, we can still conclude safely that the BDT observed in as-FIBed Si pillars is actually resulted from the FIB irradiation-introduced a-Si shell. The observed phenomena can be rationalized as below: For those as-FIBed Si pillars with $D > 400$ nm, the a-Si shell is not thick enough to absorb the elastic energy stored in the c-Si core under loading; consequently, the crack will be able to nucleate in the weakest site and then propagate across the entire sample. With the reduction of the pillar diameter, the elastic energy stored in c-Si core will become less and less and a-Si shell confinement will become more and more effective to suppress the crack nucleation and propagation, then the size-dependent BDT will be observed for as-FIBed Si pillars. The confinement from the a-Si shell was also supported by the x-ray mcirodiffraction tests[24,25] which showed that the crystalline part of the FIBed Si pillar experienced apparent strain gradient. This indicates that the a-Si shell may have some compressive effect on the pillar, which in turn helps to suppress the fracture process. However, once the a-Si shell is crystallized, the entire pillar will behave brittle again because of the absence of the confinement from the ductile a-Si shell. The mechanical properties of the pure a-Si fabricated by FIB and detailed toughening mechanisms will be discussed in a separate paper.

To address question II, we assume that FIBed Si pillars have perfect cylindrical core-shell shape with a constant a-Si shell thickness of 28 nm (see the inset schematic in Fig. 4). According to the rule of mixtures, a "composite" elastic modulus E of the core-shell structure can be calculated by neglecting the shear deformation[26]

$$E = E_c(1 - \nu_a) + E_a\nu_a, \quad (1)$$

where E_a and E_c are, respectively, the apparent elastic modulus of a-Si and c-Si, and ν_a is the volume percentage of the amorphous part in the whole pillar. Assuming that t_a being the thickness of the amorphous shell and D_c being the diameter of the c-Si core as marked in the inset in Fig. 4, Eq. (1) can be re-written as

$$E = E_c\left(\frac{D_c/2}{D/2}\right)^2 + E_a\left[1 - \left(\frac{D_c/2}{D/2}\right)\right]^2. \quad (2)$$

As $D_c = D - 2t_a$,

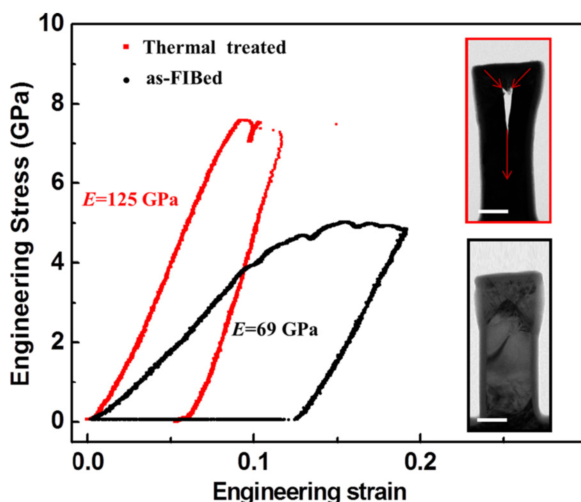

FIG. 3. Engineering stress-strain curves of a thermal-treated (red) and an as-FIBed (black) Si pillar. The insets framed by the red and black solid boxes are the postmortem bright filed TEM images of the thermal-treated and as-FIBed Si pillars, respectively. Scale bars, 100 nm.

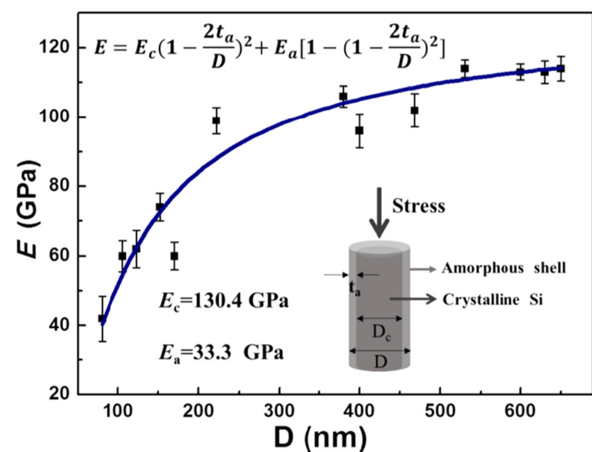

FIG. 4. Size dependence of the apparent elastic modulus of the FIBed Si pillars. The solid blue line is the linear fitting according to the equation at the top left, from which the elastic modulus of the amorphous shell and the crystalline core can be derived. The inset in the lower right is the schematic core-shell model of as-FIBed Si pillar.

This article is copyrighted as indicated in the article. Reuse of AIP content is subject to the terms at: http://scitation.aip.org/termsconditions. Downloaded to IP: 117.32.153.170 On: Wed, 04 Mar 2015 00:28:44

$$E = E_c\left(1 - \frac{2t_a}{D}\right)^2 + E_a\left[1 - \left(1 - \frac{2t_a}{D}\right)^2\right]. \qquad (3)$$

Since t_a and D are measurable parameters, only if we know E_a and E_c, E (modulus of the core-shell structured pillars) can be calculated through Eq. (3). On the other hand, because E can be measured experimentally, it is also possible to derive E_a and E_c by fitting the curve predicted by Eq. (3) to a series of real data. In order to validate this assumption, we have purposely measured the modulus of as-FIBed Si pillars with their diameter ranged from 85 nm to 650 nm. The soft "amorphous cap" on the top end of the Si pillar was pre-compacted before quantitative test to minimize its effect on the measured modulus. As shown in Fig. 4, the measured E decreased with the decreasing sample size, regardless the uncertainties in stress due to the difficulty in D determination and in strain because of the measurement errors. The best fitted curve based on Eq. (3) is plotted in Fig. 4 as a blue solid line which yielded $E_a = 33.3$ GPa and $E_c = 130.4$ GPa. The fitted value of E_c agrees well with the elastic modulus of (100) Si wafer, i.e., ∼130 GPa.[23] However, $E_a = 33.3$ GPa is much lower than the reported value (74.7 ± 12.1 GPa) of FIB-free a-Si pillars.[27] The discrepancy might be attributed to the electron beam irradiation-induced softening[28] and/or Ga ions implantation effect. It has been reported that the elastic modulus of Si nanowires with their diameters ranged from 80–600 nm was close to that of bulk Si and showed no obvious size dependency;[29] therefore, the dependence of E on D (85–650 nm) should be attributed solely to the increase of ν_a.

In summary, we have demonstrated that the size-dependent BDT of FIBed Si is actually resulted from the a-Si shell introduced during the FIB fabrication procedure instead of the intrinsic property of crystalline Si. The FIB-affected a-Si shell can be crystallized by thermal treatment, after which the Si pillars behave brittle again with their modulus and fracture strength being comparable to bulk crystalline Si. We proposed that it was the competition between the stored energy release in c-Si and the energy absorption ability of the a-Si that determined the BDT observed in FIBed Si pillars. Moreover, we have developed an analytical model which has been proved to be able to derive the E of both a-Si shell and c-Si core. Our findings suggest that it is necessary to take the FIB irradiation into consideration when the mechanical properties of FIBed small-sized Si or other semiconductor materials are investigated. Meanwhile, our findings suggest that ion bombardment-introduced soft amorphous shell layer can be used to suppress the sudden failure of micro/nanoscaled semiconductor devices in the course of service.

This research was supported by the National Natural Science Foundation of China (Nos. 51231005, 51321003, and 11132006) and the 973 Program of China under No. 2010CB631003. The authors would like to thank Boyu Liu, Penghan Lu, and Yunwei Mao at Xi'an Jiaotong University and Ju Li at Massachusetts Institute of Technology for valuable discussion.

[1]K. E. Petersen, Proc. IEEE **70**, 420 (1982).
[2]A. Blanco, E. Chomski, S. Grabtchak, M. Ibisate, S. John, S. W. Leonard, C. Lopez, F. Meseguer, H. Miguez, and J. P. Mondia, Nature **405**, 437 (2000).
[3]Q. Fang and L. Zhang, J. Mater. Res. **28**, 1995 (2013).
[4]J. Samuels and S. G. Roberts, Proc. R. S. A **421**, 1 (1989).
[5]F. Östlund, K. Rzepiejewska-Malyska, K. Leifer, L. M. Hale, Y. Tang, R. Ballarini, W. W. Gerberich, and J. Michler, Adv. Funct. Mater. **19**, 2439 (2009).
[6]Y. Zhu, F. Xu, Q. Qin, W. Y. Fung, and W. Lu, Nano Lett. **9**, 3934 (2009).
[7]T. Namazu and Y. Isono, presented at the Sixteenth Annual International Conference on Micro Electro Mechanical Systems, 2003, MEMS-03 Kyoto.
[8]S. Hoffmann, I. Utke, B. Moser, J. Michler, S. H. Christiansen, V. Schmidt, S. Senz, P. Werner, U. Gösele, and C. Ballif, Nano Lett. **6**, 622 (2006).
[9]M. J. Gordon, T. Baron, F. Dhalluin, P. Gentile, and P. Ferret, Nano Lett. **9**, 525 (2009).
[10]J. Deneen, W. M. Mook, A. Minor, W. W. Gerberich, and C. B. Carter, J. Mater. Sci. **41**, 4477 (2006).
[11]K. Kang and W. Cai, Int. J. Plast. **26**, 1387 (2010).
[12]S. Shim, H. Bei, M. K. Miller, G. M. Pharr, and E. P. George, Acta Mater. **57**, 503 (2009).
[13]R. Maaß, S. Van Petegem, H. Van Swygenhoven, P. Derlet, C. Volkert, and D. Grolimund, Phys. Rev. Lett. **99**, 145505 (2007).
[14]J. Michler, K. Wasmer, S. Meier, F. Östlund, and K. Leifer, Appl. Phys. Lett. **90**, 043123 (2007).
[15]Z. W. Shan, G. Adesso, A. Cabot, M. P. Sherburne, S. A. Syed Asif, O. L. Warren, D. C. Chrzan, A. M. Minor, and A. P. Alivisatos, Nat. Mater. **7**, 947 (2008).
[16]A. Minor, J. Ye, C. Chisholm, R. Mishra, Z. Shan, and O. Warren, Microsc. Microanal. **15**, 1184 (2009).
[17]S. Korte, J. S. Barnard, R. J. Stearn, and W. J. Clegg, Int. J. Plast. **27**, 1853 (2011).
[18]S. E. Donnelly, R. C. Birtcher, V. M. Vishnyakov, and G. Carter, Appl. Phys. Lett. **82**, 1860 (2003).
[19]I. Jenčič and I. M. Robertson, J. Mater. Res. **11**, 2152 (1996).
[20]F. Priolo, A. Battaglia, R. Nicotra, and E. Rimini, Appl. Phys. Lett. **57**, 768 (1990).
[21]M. K. Hatalis and D. W. Greve, IEEE Electron Device Lett. **8**, 361 (1987).
[22]K. Nakazawa, J. Appl. Phys. **69**, 1703 (1991).
[23]M. A. Hopcroft, W. D. Nix, and T. W. Kenny, J. Microelectromech. Syst. **19**, 229 (2010).
[24]R. Maaβ, D. Grolimund, S. Van Petegem, M. Willimann, M. Jensen, H. Van Swygenhoven, T. Lehnert, M. A. M. Gijs, C. A. Volkert, and E. T. Lilleodden, Appl. Phys. Lett. **89**, 151905 (2006).
[25]R. Maaß, S. Van Petegem, C. N. Borca, and H. Van Swygenhoven, Mater. Sci. Eng. A **524**, 40 (2009).
[26]F. G. Sen, Y. Qi, A. C. T. van Duin, and A. T. Alpas, Appl. Phys. Lett. **102**, 051912 (2013).
[27]Q. P. McAllister, K. E. Strawhecker, C. R. Becker, and C. A. Lundgren, J. Power Sources **257**, 380 (2014).
[28]K. Zheng, C. Wang, Y. Q. Cheng, Y. Yue, X. Han, Z. Zhang, Z. Shan, S. X. Mao, M. Ye, Y. Yin, and E. Ma, Nat. Commun. **1**, 24 (2010).
[29]Y.-S. Sohn, J. Park, G. Yoon, J. Song, S.-W. Jee, J.-H. Lee, S. Na, T. Kwon, and K. Eom, Nanoscale Res. Lett. **5**, 211 (2010).
[30]See supplementary material at http://dx.doi.org/10.1063/1.4913241 for movie S1 that recored the *in situ* compression of the as-FIBed Si pillar with D = 212 nm in TEM, and movie S2 of the compression of the D = 206 nm thermal-treated Si pillar inside TEM.

This article is copyrighted as indicated in the article. Reuse of AIP content is subject to the terms at: http://scitation.aip.org/termsconditions. Downloaded to IP: 117.32.153.170 On: Wed, 04 Mar 2015 00:28:44